Mass-Conservative Transport of Atmospheric Constituents

Second Lecture (# 7)

by

Bennert Machenhauer, DMI

”Exact” departure cell (red rectangle) and backward trajectories (blue lines) for the analytical velocity field consisting of a translational, a divegent and a rotational part.

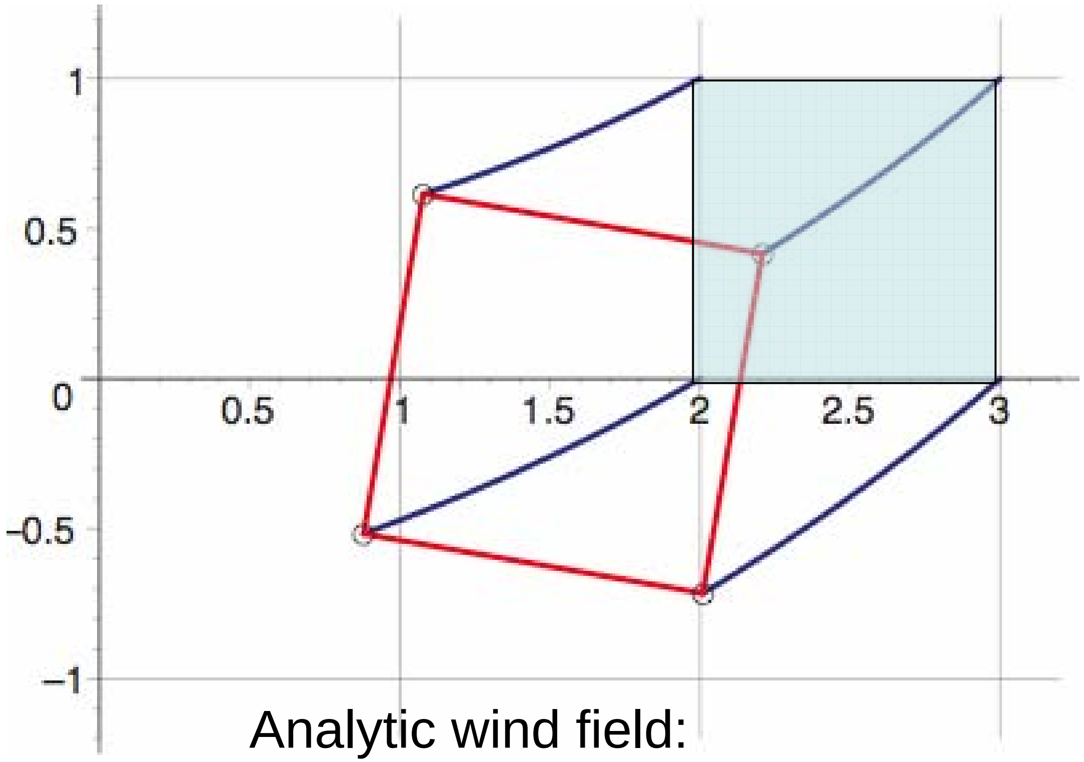

Analytic wind field:

$$u(x,y) = u_0 + D_0 x - R_0 y; \quad (u_0, v_0) = 54\,(\cos(10\,\mathrm{deg}), \cos(10\,\mathrm{deg}))\; m/s$$

$$v(x,y) = v_0 + D_0 y + R_0 x. \quad D_0 = -0.0023\, s^{-1}; R_0 = 0.0029\, s^{-1};$$

Graphical illustration of the departure areas for different DCISL schemes for the idealized test case for assessing the degree of local mass conservation.
The read rectangle is the exact departure area.

RANCIC [1992]

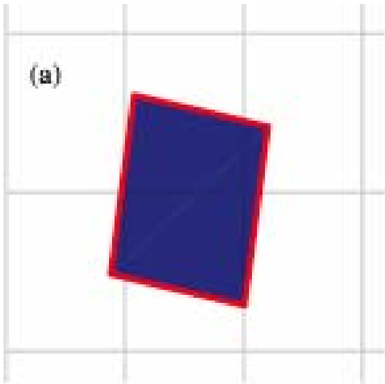

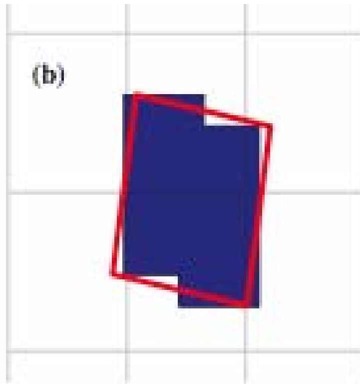

MACHENHAUER and OLK [1998]

NAIR et al. [2002]

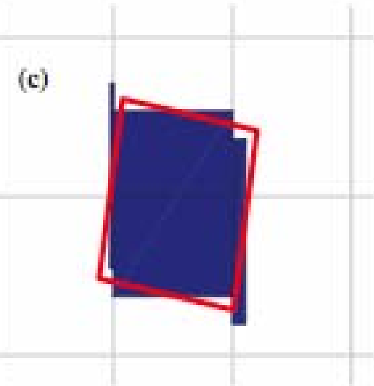

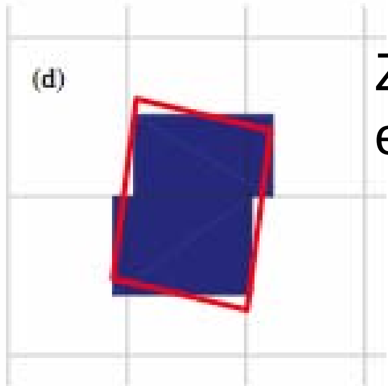

ZERROUKAT et al. [2002]

COLLINS ET AL. (2004) (LINN and ROOD [1996]):

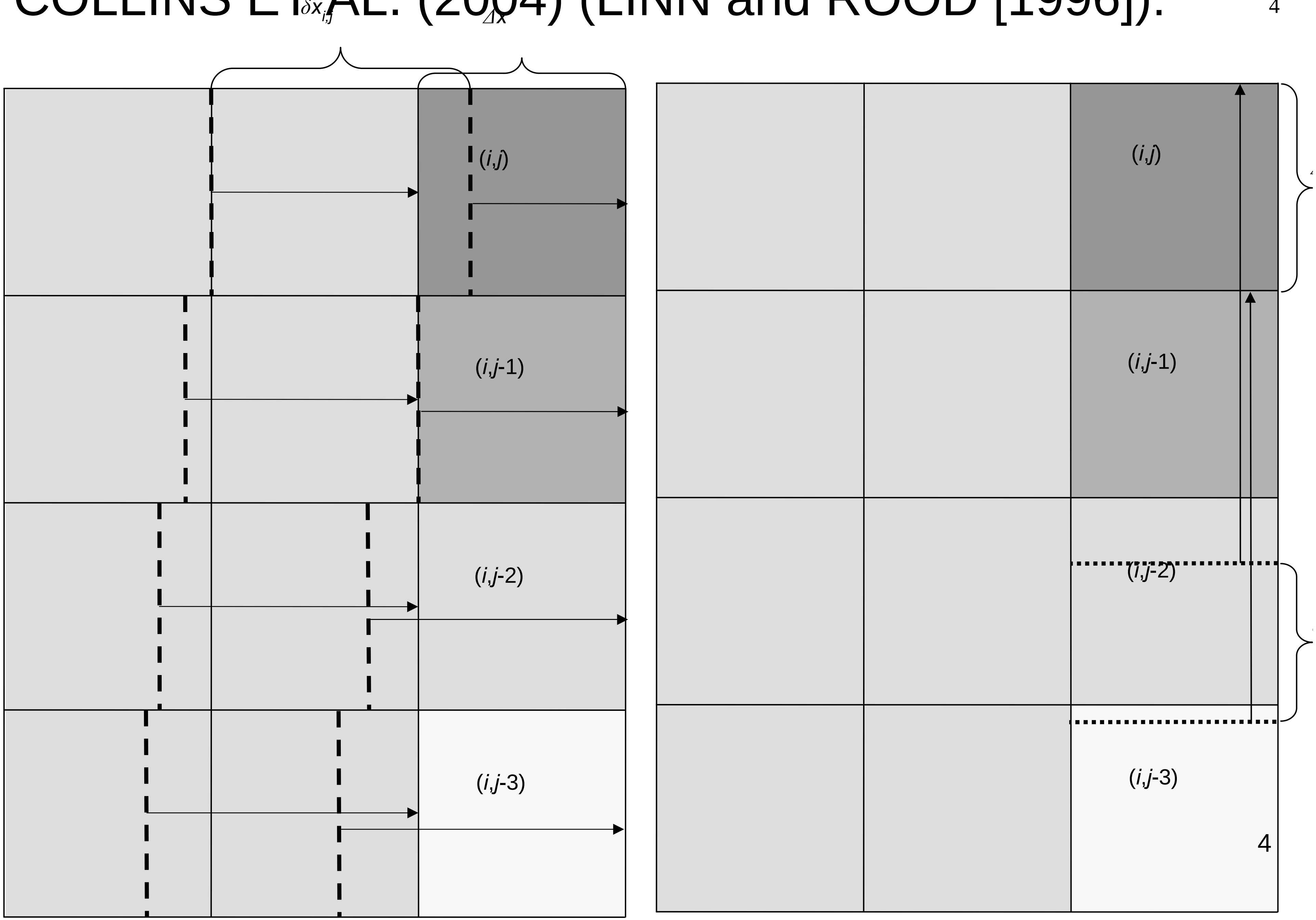

Graphical illustration of the FFSL scheme (LINN and ROOD [1996]) for the idealized test case for assessing the degree of local mass conservation. The read rectangle is the exact departure area.

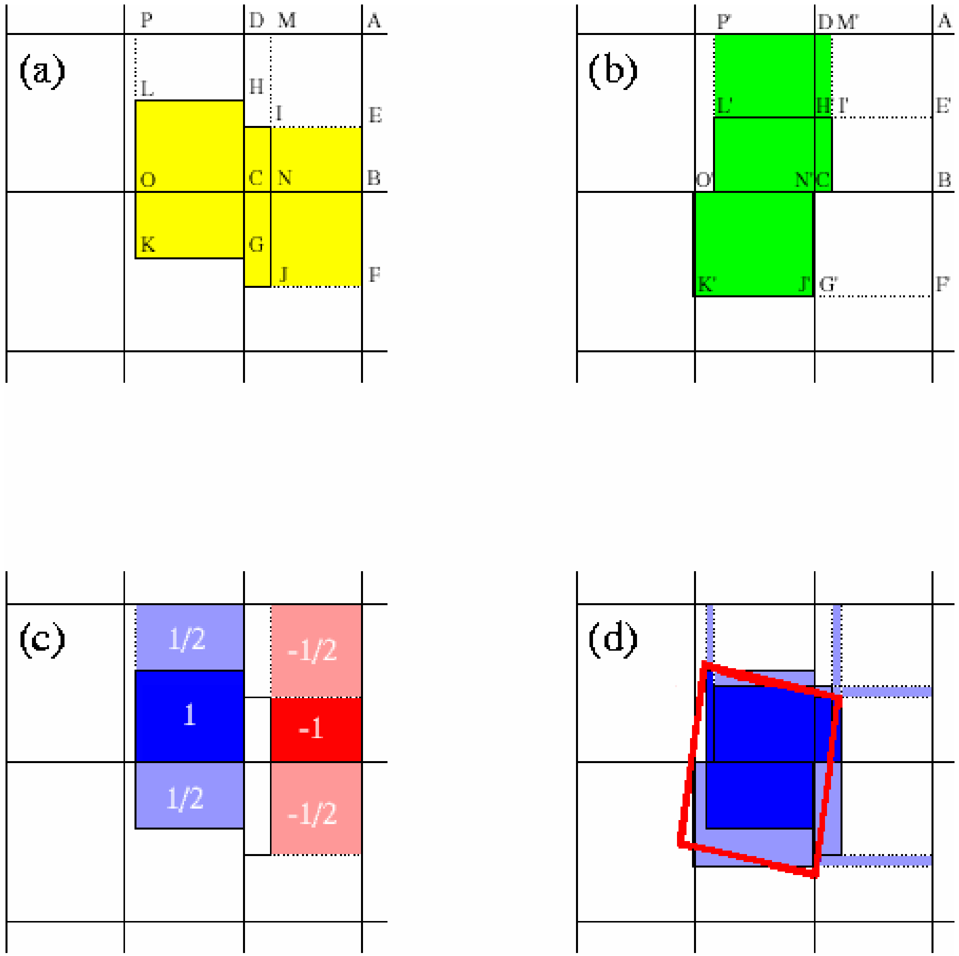

d) Shows the effective departure area: =100% = 50%

The monotonic filter of COLELLA, P., WOODWARD, P. R. (1984). Piecewise parabolic method for gas-dynamical simulations. *J. Comp. Phys.,* **54**, 174–201.

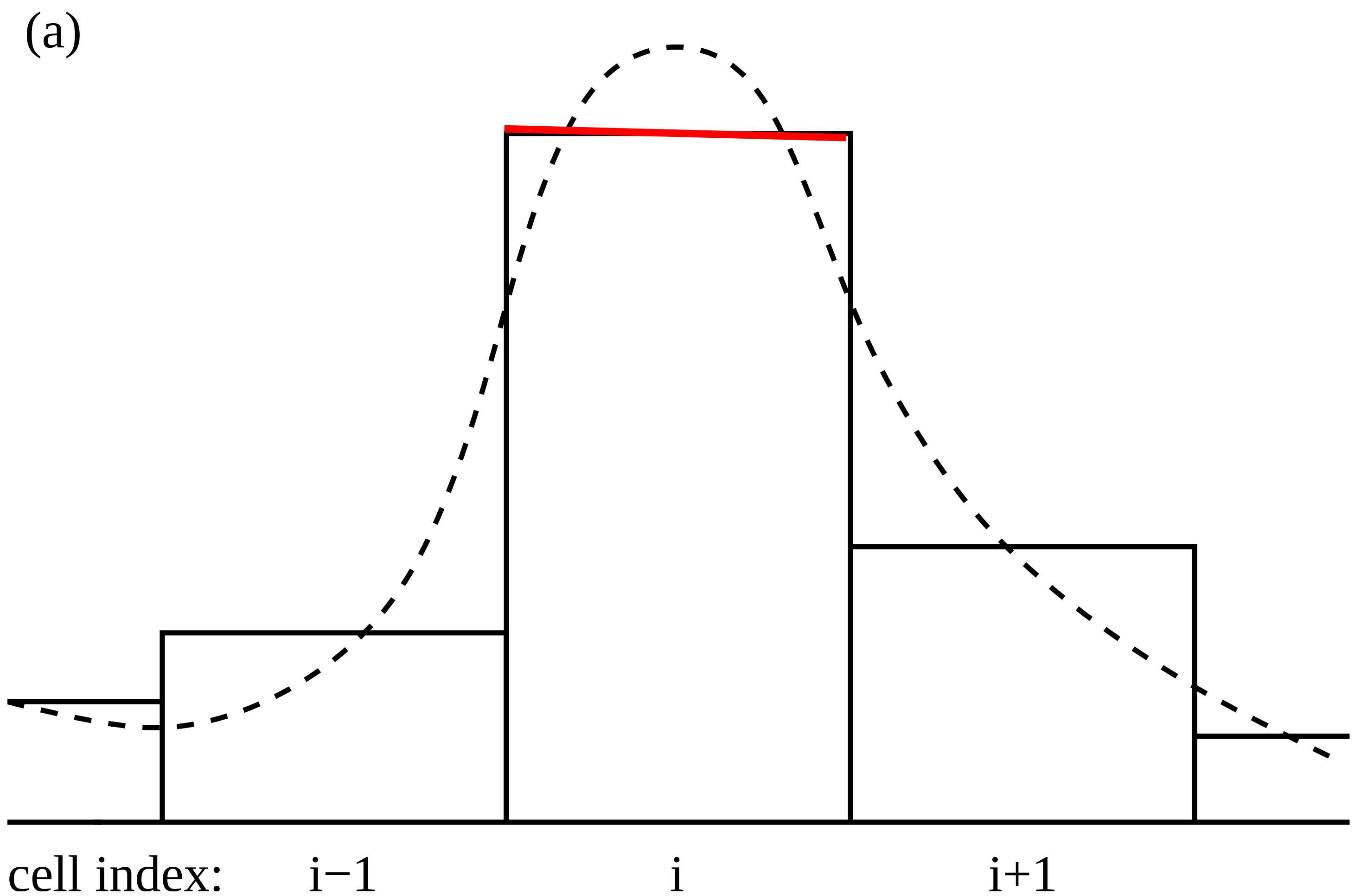

COLELLA, P., WOODWARD, P. R. (1984). Piecewise parabolic method for gas-dynamical simulations. *J. Comp. Phys.*, **54**, 174–201.

(b)

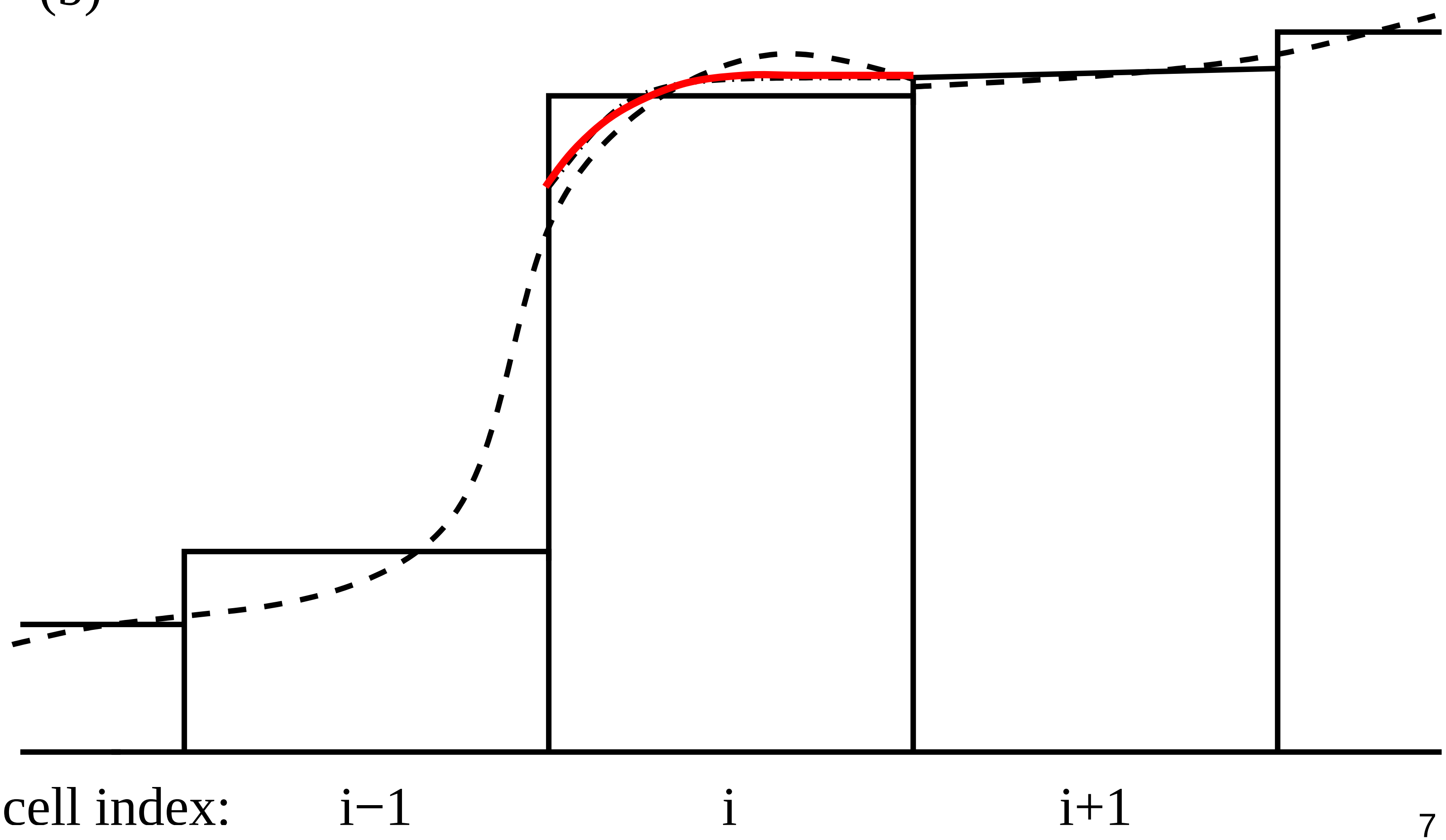

Tests and results

Error measures:

$$rms = \sqrt{\frac{1}{K}\sum_{k=1}^{K}\left(\psi_k - \psi_k^t\right)^2} \quad , \qquad l_1 = \frac{\sum_{k=1}^{K}\left|\psi_k - \psi_k^t\right|}{\sum_{k=1}^{K}\left|\psi_k^t\right|} \quad ,$$

$$l_2 = \frac{\sqrt{\sum_{k=1}^{K}\left(\psi_k - \psi_k^t\right)^2}}{\sqrt{\sum_{k=1}^{K}\left(\psi_k^t\right)^2}} \quad , \qquad l_\infty = \frac{\max\left(\left|\psi_k - \psi_k^t\right|\right)}{\max\left(\left|\psi_k^t\right|\right)}$$

$$h_{max} = \frac{\max(\psi) - \max(\psi^t)}{S^t} \quad \text{and} \quad h_{min} = \frac{\min(\psi) - \min(\psi^t)}{S^t}$$

$$\text{with} \quad S^t = \max(\psi^t) - \min(\psi^t)$$

ψ_k^t is the analytical (true) value in grid point k

The monotonic filter of COLELLA and WOODWARD (1984) A (SOLID BODY EXPREIMENTS)

	$\hat{\alpha} = 0$			$\hat{\alpha} = \pi / 2$			$= \pi/3$		
Schemes	l_1	l_2	l_∞	l_1	l_2				
SLICE-N	0.046	0.029	0.022	0.079	0.049	0.042	—	—	—
SLICE-M	0.038	0.024	0.017	0.058	0.040	0.037	—	—	—
CISL-N	**0.052**	**0.035**	**0.032**	**0.063**	**0.046**	**0.048**	**0.075**	**0.051**	**0.083**
CISL-P	0.025	0.025	0.031	0.059	0.045	0.048	0.043	0.082	0.076
CISL-M	**0.094**	**0.091**	**0.108**	**0.084**	**0.084**	**0.109**	**0.077**	**0.089**	**0.18**
CCS-N	—	—	—	**0.054**	**0.042**	**0.065**	**0.051**	**0.039**	**0.076**
CCS-P	0.036	0.034	0.042	0.051	0.041	0.065	0.033	0.034	0.077
CCS-M			—	**0.076**	**0.082**	—	—	**0.086**	**0.186**

A situation in which the unmodified sub-grid-cell reconstruction exhibits strong Gibbs phenomen

Semi-monotonic filter of LIN and ROOD [1996].

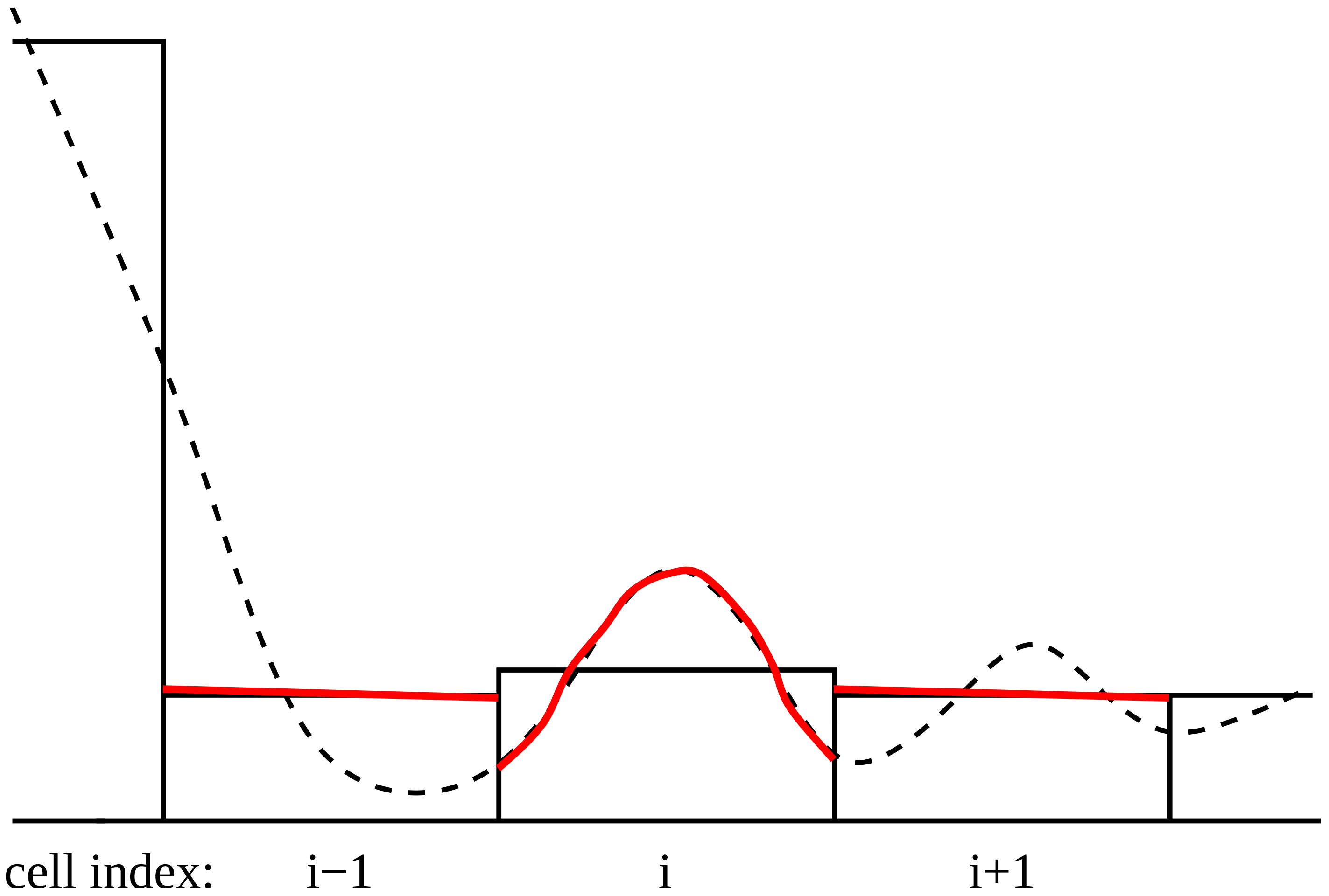

The positive-definite filter of LIN and ROOD [1996];

							= $\pi/3$		
Schemes									
SLICE-N	0.046	0.029	0.022	0.079	0.049	0.042	—	—	—
SLICE-M	0.038	0.024	0.017	0.058	0.040	0.037	—	—	—
CISL-N	**0.052**	**0.035**	**0.032**	**0.063**	**0.046**	**0.048**	**0.075**	**0.051**	**0.083**
CISL-P	**0.025**	**0.025**	**0.031**	**0.059**	**0.045**	**0.048**	**0.043**	**0.082**	**0.076**
CISL-M	0.094	0.091	0.108	0.084	0.084	0.109	0.077	0.089	0.18
CCS-N	—	—	—	**0.054**	**0.042**	**0.065**	**0.051**	**0.039**	**0.076**
CCS-P	**0.036**	**0.034**	**0.042**	**0.051**	**0.041**	**0.065**	**0.033**	**0.034**	**0.077**
CCS-M	—	—	—	0.076	0.082	0.129	0.070	0.086	0.186

A simple and efficient locally mass conserving semi-Lagrangian transport scheme

By EIGIL KAAS*
Niels Bohr Institute, University of Copenhagen, Denmark

(Manuscript received 7 August 2007; in final form XX XXXXXX 200X)

ABSTRACT

A new simple and accurate locally mass conserving semi-Lagrangian (LMCSL) scheme has been constructed. Mass conservation is obtained by introducing modified interpolation weights at the upstream departure points. Thereby the total mass given off by a given Eulerian grid point to all the surrounding semi Lagrangian (SL) departure points is equal to the cell area represented by that grid point. The new scheme is equivalent to the cell-integrated semi-Lagrangian (CISL) transport schemes in the sense that divergence - via the weights - is determined by the trajectories and not by centred differences as in traditional SL-schemes.

The LMCSL scheme has been combined with the semi-implicit scheme in a shallow water model. Thereby a numerically stable and inherently mass conserving scheme permitting long time steps has been set up. Tests in plane horizontal geometry including topography give solutions very similar to those obtained with the traditional semi-implicit SL scheme. The well known mountain wave resonance problem appears to be reduced.

The increase in numerical cost of the new scheme relative to traditional SL models is small, particularly when there are several passive tracers, since the same weights are used for all tracers.

1 Introduction

New generations of atmospheric circulation models for use in numerical weather prediction (NWP) and climate research include the individual densities of an increasing number of particles and chemical tracers, as prognostic variables. These variables are introduced to be able, in a consistent way, to forecast and simulate the evolution of air pollution and air chemistry, to simulate the direct radiative effects of the tracer constituents, and to simulate the indirect effects of some particles (CCN's) on cloud microphysics. By consistent is here meant that the evolution of the chemical constituents are based on the same numerical techniques and with the same resolution in both time and space as the physical model. Consistency is of importance for obtaining accurate simulations of one and two-way interactions between the physical atmosphere (including clouds and precipitation) and atmospheric chemistry. The issue of model internal consistency has been discussed in detail in Jöckel et al. (2001).

Rasch and Williamson (1990) have defined seven desirable properties for transport schemes, i.e. numerical schemes designed for solving the continuity equation: accuracy, stability, computational efficiency, transportivity, locality, conservation and shape-preservation.

Obviously, accuracy and computational efficiency are inter-related since in real applications, where the computer resource is given, it often pays off to enhance the spatial resolution, i.e. the number of grid points, at the expense of the formal numerical accuracy. Also stability can be related to computational efficiency: e.g. semi implicit (SI) integration schemes (Robert et al. (1972)) are known for their high numerical stability even for long time steps. However, SI-schemes involve the solution of an elliptic equation, and this is generally less efficient on massive parallel computers due to considerable data-interchange between the computational nodes.

The transportivity and locality properties of a scheme refer to its ability to transport information along the characteristics, and that only adjacent grid points affect the forecast at a given point. ... Lagrangian ... semi-Lagrangian and semi-... schemes, and by definition ... "transportive" ... spectral models are non-local.

Formal conservation ... important for atmospheric constituents with a relatively long residence time in the atmosphere. The notion "local mass conservation" refers to the

* Corresponding author.
e-mail: kaas@nbi.ku.dk

KAAS, E. (2008). A simple and efficient locally mass conserving semi-Lagrangian transport scheme. *Tellus A*, In press.

The Continuity Equation

<u>Continuity equation for passive tracer or for air (q=1), Eulerian formulation</u>

$$\frac{\partial \psi}{\partial t} = -\nabla \cdot \boldsymbol{v}\psi \qquad (\psi = q\rho \quad \text{density})$$

<u>Continuity equation for passive tracer or for air, Lagrangian formulation</u>

$$\frac{d\psi}{dt} = -\psi \nabla \cdot \boldsymbol{v}$$

Traditional semi-Lagrangian (SL) scheme

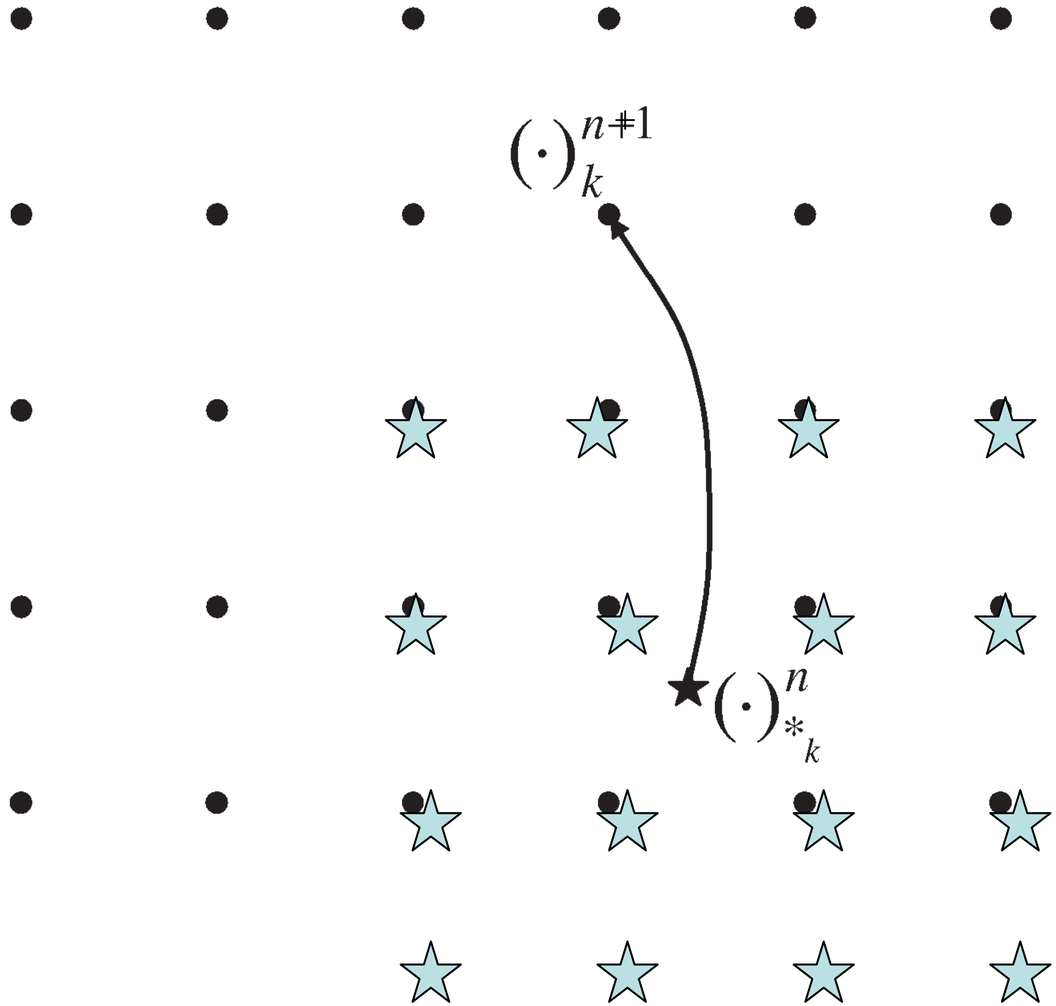

Traditional semi-Lagrangian (SL) scheme

Explicit forecast in grid point *k* :

$$\psi_{k\ \mathrm{SL\text{-}exp}}^{n+1} = \psi_{*_k}^{n} - 0.5\Delta t\left\{\left(\psi\nabla\cdot\boldsymbol{v}\right)_{*_k}^{n} + \left(\tilde{\psi}\nabla\cdot\boldsymbol{v}\right)_{k}^{n+1}\right\}$$

$$= \sum_{l}^{K} w_{k,l}\left(\psi_l^n - 0.5\Delta t\left(\psi\nabla\cdot\boldsymbol{v}\right)_l^n\right) \quad - 0.5\Delta t\left(\tilde{\psi}\nabla\cdot\boldsymbol{v}\right)_k^{n+1}$$

$$\sum_{l=1}^{K} w_{k,l} = 1 \qquad \left(\sum_{k=1}^{K} w_{k,l} = 1 \quad \mathit{for\ non-divegent\ \ flow}\right)$$

k Grid point/cell index. $k = 1, \ldots, K, \quad K = nlon \times nlat$

l Grid point/cell index. $l = 1, \ldots, K.$

$w_{k,l}$ Interpolation weight on upstream grid point (l) surrounding the departure grid point (k).

$$(\square)^{n+1}$$

$$(\square)^{n+1} = 2(\square)^{n} - (\square)^{n-1}$$

LMCSL

A new simple locally mass conserving semi-Lagrangian (LMCSL) transport scheme

"Based on cell-integrated semi-Lagrangian (CISL) thinking"

:

Explicit forecast in grid point *k:*

$$\overline{\psi}_k^{n+1}{}_{\text{LM-exp}} = \left\{\overline{\psi}\right\}^n_{**k}$$

$$\equiv \sum_{l=1}^{K} \hat{w}_{k,l}\overline{\psi}_l^n \quad \text{where} \quad \hat{w}_{k,l} = \frac{A_l}{A_k}\frac{w_{k,l}}{\sum_{m=1}^{K} w_{m,l}}$$

A_k is the volume represented by the *k*th Eulerian grid point.

$$\left(\sum_{k=1}^{K} w_{k,l} = 1 \quad \textit{for non-divegent flow}\right)$$

LCISL scheme:
Mass contributing grid points with bi-parabolic interpolation

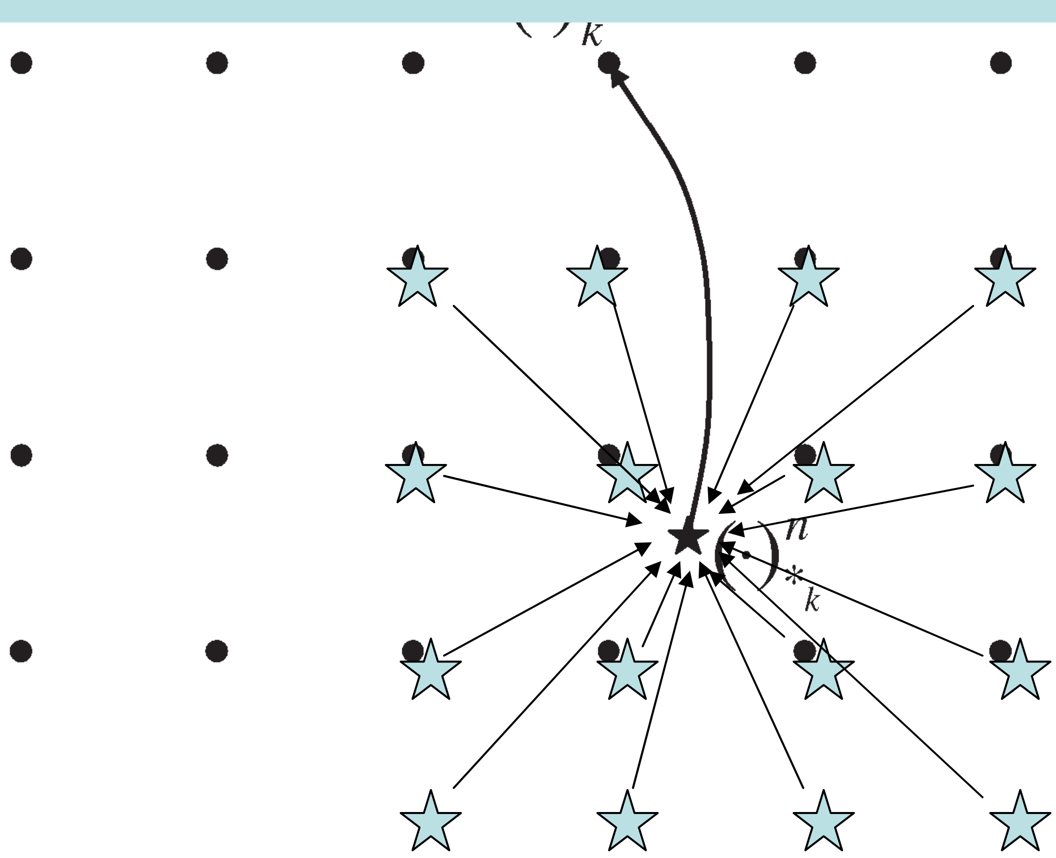

”Departure area” for one-dimensional LMCSL scheme based on parabolic interpolation. (Non-divergent case)

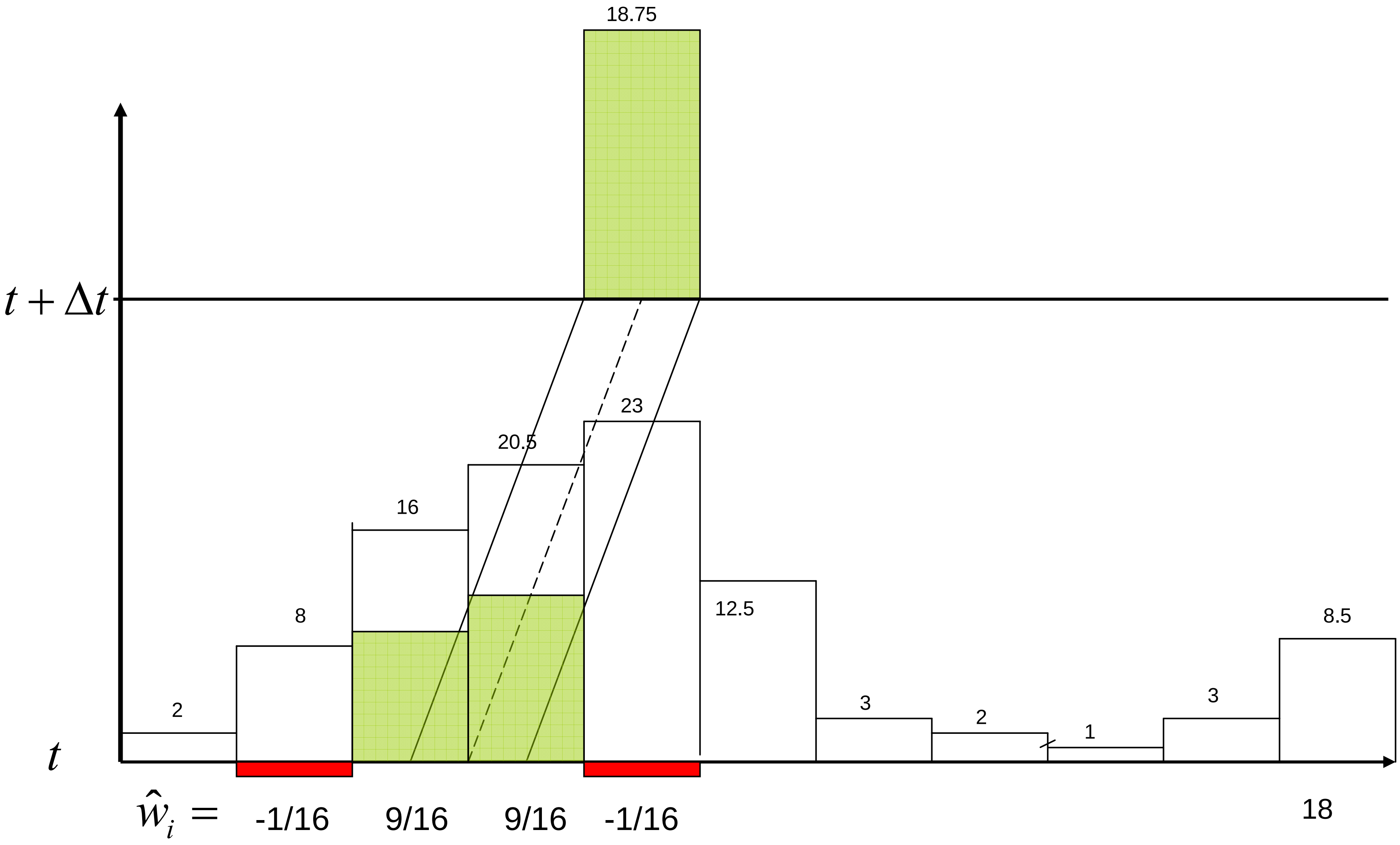

”Departure area” for the LMCSL scheme based on bi-parabolic interpolation

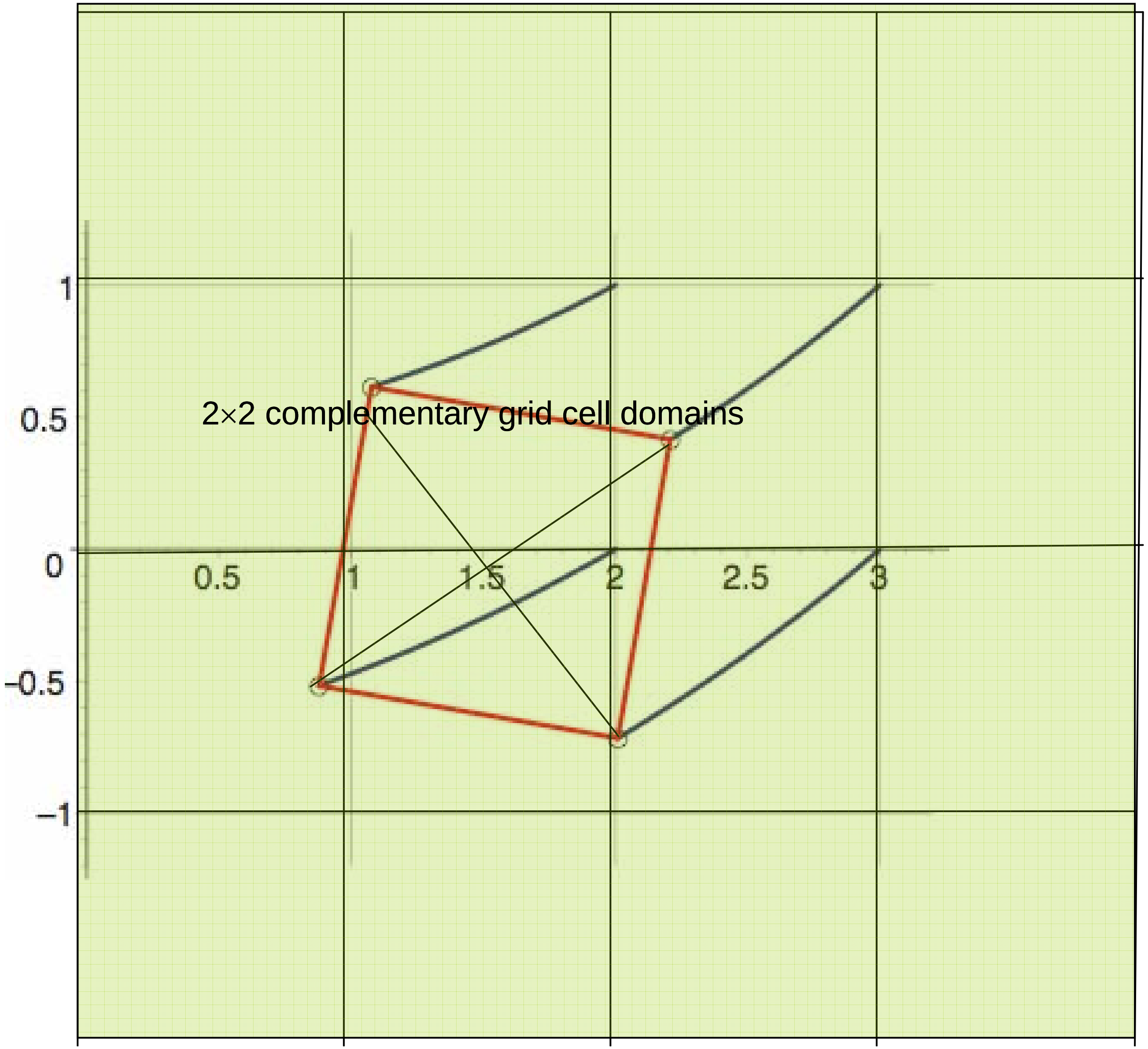

Monotonic and positive-definite filter by KAAS (2008)

– a posteriori correction

Input to filter:

- A high order (bi-cubic interpolation) LMCSL unfiltered forecast ψ.
- A low order (bi-linear interpolation) LMCSL unfiltered forecast ψ_L
- A maximum (ψ_{max}) and minimum (ψ_{min}) value permitted in each grid cell. This is defined from the maximum and minimum values of the four upstream grid points surrounding the semi-Lagrangian departure point, and modified by the effect of divergence/convergence. Divergence is taken into account using the traditional centered difference definition of divergence, implying that the filter ensures conservation of a constant field in non-divergent flows (assuming the centred difference way of defining divergence).

The filter:

The filter includes the following steps:

1. Set target values ψ_T equal to ψ.
2. Identify grid cells where $\psi_T \notin [\psi_{min}, \psi_{max}]$. In these and in the eight neighboring grid cells a mask is set.
3. In the masked cells (and only in these) a modified anti-diffused target value is set:

   $\psi_T = \psi + a\,(\psi - \psi_L)$; with $a = \min(0.7, 1000.\times((\psi - \psi_L)/r)^2)$ and

   $r = \max(\psi) - \min(\psi)$. The maximum and minimum values can be over the entire domain or over a sub-domain. In the present application it is taken over a 9 by 9 grid point domain surrounding the actual cell. Such regional maximum and minimum values can be calculated efficiently.

Monotonic and positive definite filter (continued)

The main motivation for the choice of target value is that the smallest scales should be antifiltered most strongly. Note that $((\psi - \psi_L)/r)^2$ is generally large for small scales and small for large scales. It can in fact be demonstrated that a non-linear antidiffusion of the proposed type will improve also a classical semi-Lagrangian forecast when applied in all grid points.

4. In the masked cells the target values, ψ_T, are reset to $\min(\psi_{max},\max(\psi_{min},\psi_T))$ to ensure shape conservation.

5. The ψ values in 2×2 complementary grid cell domains covering the total integration domain are modified to ensure new ψ values which are as close as possible to ψ_T under the strong constraint of local conservation of total mass in the four grid cells and the weak constraint of limitation to the individual grid cell intervals $[\psi_{min}, \psi_{max}]$. Generally most 2×2 domains are unchanged since $\psi_T = \psi$.

Monotonic and positive definite filter (continued)

6. The above step is repeated for the set of 2×2 complementary grid cell domains that provide maximum spatial overlaps with the domains in the previous step.

7. A final check and correction for violation of $\psi \in [\psi_{min}, \psi_{max}]$ is done on slightly larger grid cell domains (up to 13×13 grid cells) surrounding the violating cell using the same procedure as above for the 2×2 domains. This step only becomes active around very few – if any – violating cells.

Tests and results

Error measures:

$$rms = \sqrt{\frac{1}{K}\sum_{k=1}^{K}\left(\psi_k - \psi_k^t\right)^2} \quad , \qquad l_1 = \frac{\sum_{k=1}^{K}\left|\psi_k - \psi_k^t\right|}{\sum_{k=1}^{K}\left|\psi_k^t\right|} \quad ,$$

$$l_2 = \frac{\sqrt{\sum_{k=1}^{K}\left(\psi_k - \psi_k^t\right)^2}}{\sqrt{\sum_{k=1}^{K}\left(\psi_k^t\right)^2}} \quad , \qquad l_\infty = \frac{\max\left(\left|\psi_k - \psi_k^t\right|\right)}{\max\left(\left|\psi_k^t\right|\right)}$$

$$h_{max} = \frac{\max(\psi) - \max(\psi^t)}{S^t} \quad \text{and} \quad h_{min} = \frac{\min(\psi) - \min(\psi^t)}{S^t}$$

$$\text{with} \quad S^t = \max(\psi^t) - \min(\psi^t)$$

ψ_k^t is the analytical (true) value in grid point k

Tests and results

Application to the shallow water equations and the semi-implicit technique

$$\frac{du}{dt} = fv - \frac{d(\varphi + \varphi_s)}{dx}$$

$$\frac{dv}{dt} = -fu - \frac{d(\varphi + \varphi_s)}{dy}$$

$$\frac{d\varphi}{dt} = -\varphi D + F_\varphi \quad , \qquad D = \nabla \cdot \boldsymbol{v} = \frac{du}{dx} + \frac{dv}{dy}$$

$$\frac{d\psi}{dt} = -\psi D \qquad ,$$

$$\text{where} \quad \begin{cases} \varphi & = gh, \quad h \text{ is depth of fluid} \\ \varphi_s & = gh_s, \quad h_s \text{ is height of topography} \\ u, v & \text{velocity components} \\ F_\varphi & \text{Newtonian cooling (driving the model)} \\ \psi & \text{density of passive tracer} \end{cases}$$

Tests and results

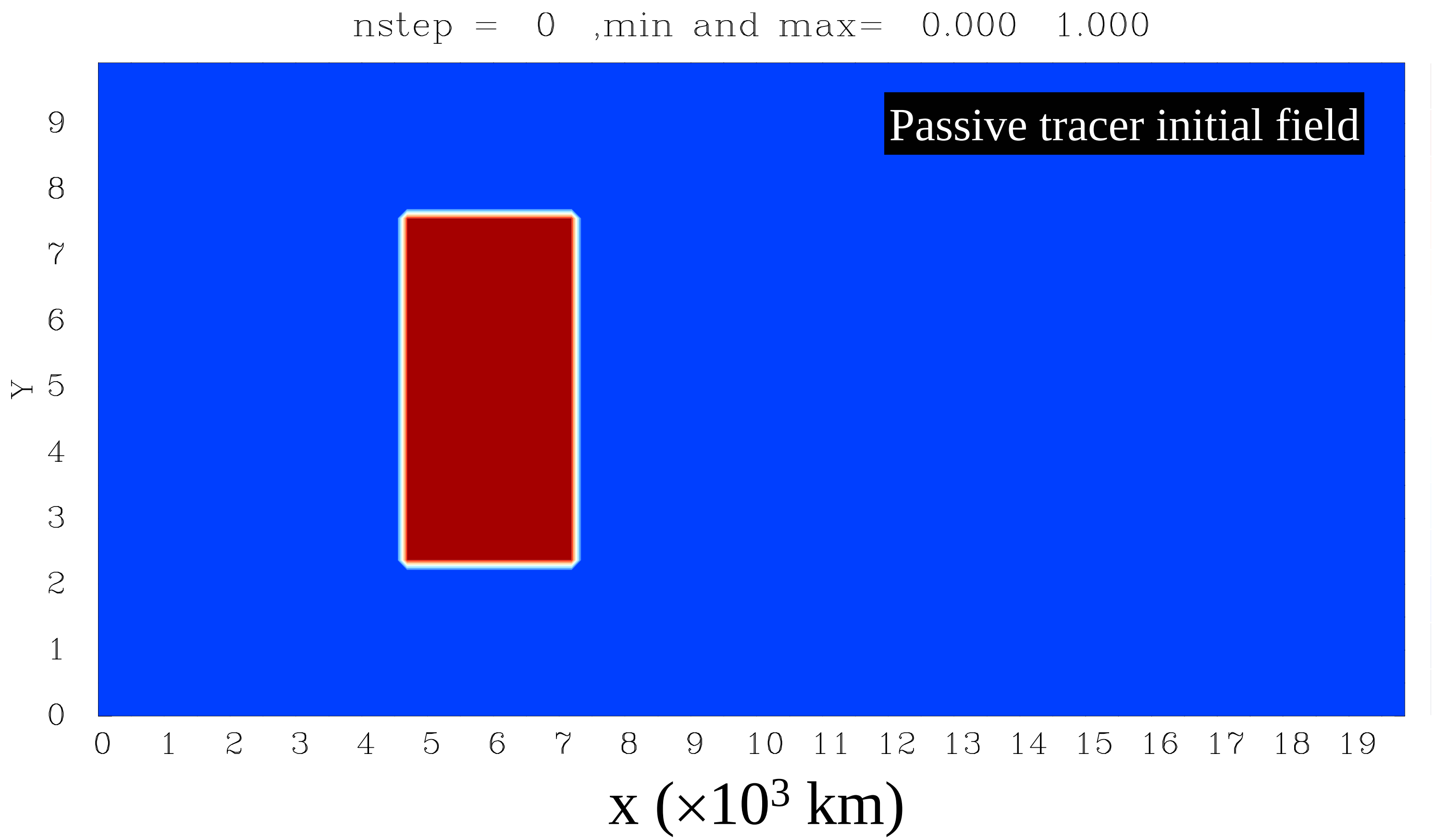

Tests and results

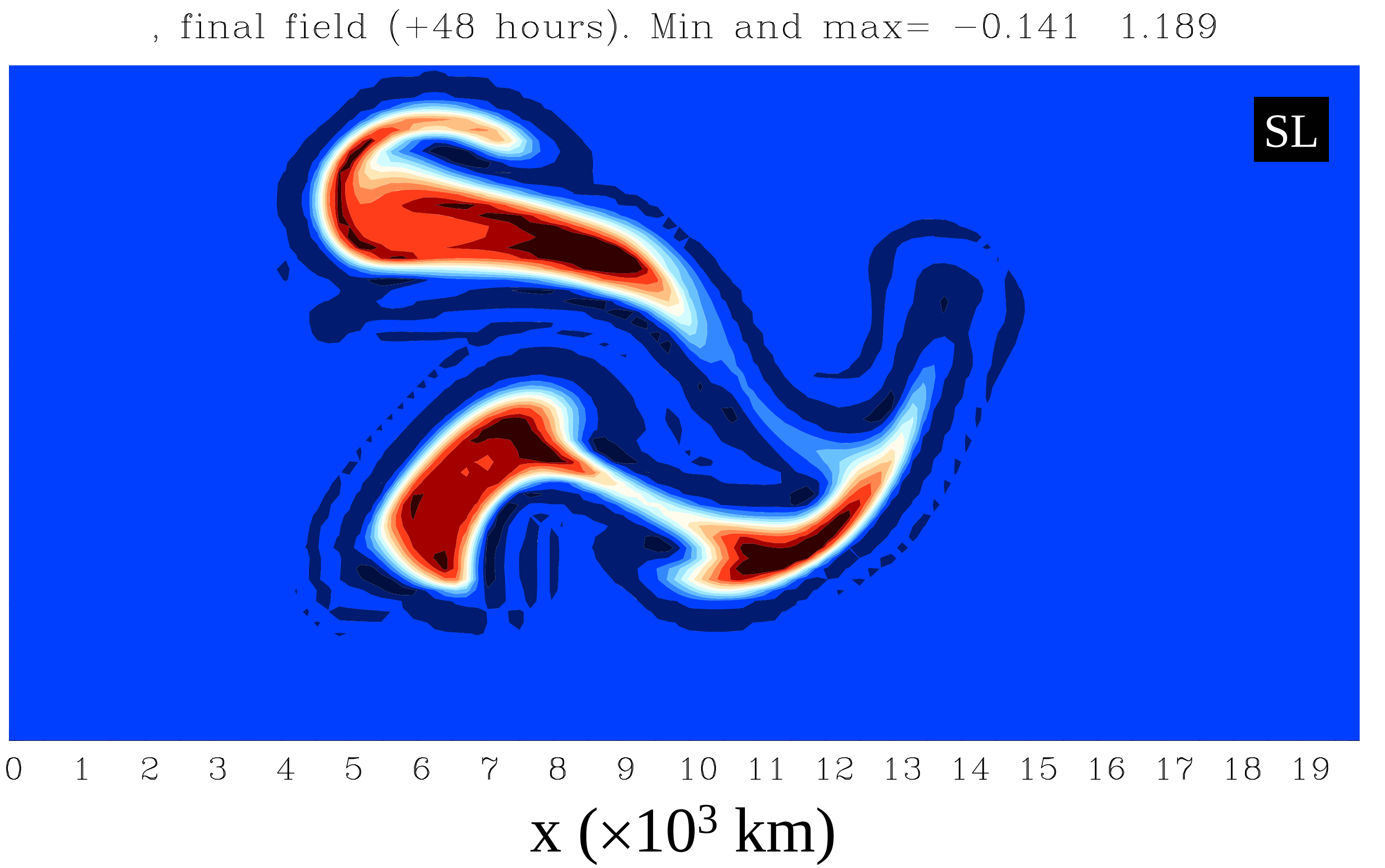

Tests and results